Expanded Coverage of Phytocompounds by Mass Spectrometry Imaging Using On-Tissue Chemical Derivatization by 4-APEBA

Kevin J. Zemaitis,[a] Vivian Lin,[a] Amir H. Ahkami,[a] Tanya Winkler,[a] Christopher R. Anderton,[a] and Dušan Veličković*[a]

Earth and Biological Sciences Directorate, Pacific Northwest National Laboratory, Richland, WA, 99354, USA

ABSTRACT: Probing the entirety of any species metabolome is an analytical grand challenge, especially at a cellular scale. Matrix-assisted laser desorption/ionization mass spectrometry imaging (MALDI-MSI) is a common spatial metabolomics assay, but this technique has limited molecular coverage for several reasons. To expand the application space of spatial metabolomics, we developed an on-tissue chemical derivatization (OTCD) workflow using 4-APEBA for confident identification of several dozen elusive phytocompounds. Overall, this new OTCD method enabled the annotation of roughly 280 metabolites, with only 10% overlap in metabolic coverage when compared to analog negative ion mode MALDI-MSI on serial sections. We demonstrate that 4-APEBA outperforms other derivatization agents providing: (1) broad specificity towards carbonyls, (2) low background, and (3) introduction of bromine isotopes. Notably, the latter two attributes also facilitate more confidence in our bioinformatics for data processing. The workflow detailed here trailblazes a path towards spatial hormonomics within plant samples, enhancing detection of carboxylates, aldehydes, and plausibly other carbonyls. As such, several phytohormones, which have various roles within stress responses and cellular communication can now be spatially profiled, as demonstrated in poplar root and soybean root nodule.

There are an estimated 200,000 to 1,000,000 distinct metabolites in the plant kingdom, where any single plant species can produce tens of thousands of unique metabolites, far more than most other organisms.[1] However, only about 14,000 metabolites in the plant kingdom have been characterized, suggesting that advanced analytical methods are needed to more thoroughly investigate such highly complex metabolomes.[2] This issue is further compounded when considering metabolite levels within single cells, where volumes and quantities of analytes are low and generally detection is limited to only a small set of compounds.[3] Significant advancements in spatially-resolved and cell-specific metabolomics have emerged in the last decade,[3, 4] and the use of these technologies have suggested a central role of cellular heterogeneity in biological systems (including plants) under different conditions where bulk measurements often mask relevant mechanistic insights.[3] One of the most utilized techniques for targeting and unveiling the cell-specific molecular signatures is matrix-assisted laser desorption/ionization (MALDI) mass spectrometry imaging (MSI).[4] MALDI-MSI has been applied for spatio-chemical analysis of polysaccharides,[5] glycans,[6] lipids,[7] proteins[8] and their proteoforms,[9] and various primary[10] and secondary metabolites[11] in plants.

Although widely applied in plant systems, a significant challenge remains in the ability of MALDI-MSI to measure and map many important phytocompounds. The lack of sensitivity towards these compounds is due, in part, to several factors that include their low mass, low abundance, low ionization yield, and tissue suppression effects. All of these limits the ability of current approaches to comprehensively describe the molecular makeup at the single cell level.[12] An additional challenge is that the broad physicochemical diversity of plant metabolites hinders their global analysis within any singular MSI workflow (e.g., using a single MALDI matrix, polarity, or mass range), and more comprehensive approaches have to be taken for broader utility of MALDI-MSI.

Recently, on-tissue chemical derivatization (OTCD) coupled with MALDI-MSI has emerged as a powerful approach to overcome sensitivity and other mass analyzer limitations.[12-15] This approach enables visualization of the spatial distribution of many biological compounds and molecular networks in microbial, plant, and mammalian cells.[16] Specifically, OTCD enhances the detection sensitivity by introducing a charged moiety or a readily ionizable functional group to the analyte. Concurrently, this derivatization process increases masses of the metabolites toward more sensitive regions, bypassing issues related to discrimination of metabolites from complex background spectral features (i.e., isobaric separation) and low mass transmission limitations of high-resolution mass spectrometers, such as Fourier transform ion cyclotron resonance mass spectrometry (FTICR-MS) instruments.

Various derivatization agents (DA) have been developed to target distinct functional groups of endogenous molecules.[12, 13] For example, Girard's T (GT), Girard's P (GP), coniferyl alcohol (CA), and 2-picolyamine (PA) have been used for OTCD of carbonyl, amine, and carboxyl-containing compounds, respectively, in plant tissues, which enabled the detection of over six hundred unique metabolite features.[17, 18] While OTCD approaches with

these DAs is promising, many challenges remain. For example, phytocompounds, including phytohormones, remain largely undetectable. Another issue is that the chemical composition of these DAs does not permit the ability to confidently distinguish between derivatized and non-derivatized MS signals.[17, 19] Moreover, since many of these DAs are highly specific, it requires the use of multiple DAs to detect chemically diverse metabolites within a single analysis.

Herein, we report an OTCD strategy using 4-(2-((4-bromophenethyl)dimethylammonium)ethoxy) benzenaminium dibromide (4-APEBA), which we found surpassed the benefits of conventional DAs used for carboxyl and aldehyde derivatization. These three chemical moieties cover a very broad metabolic space, with a vast majority of plant metabolites containing at least one of these functional groups. 4-APEBA was initially introduced for electrospray ionization (ESI) workflows for derivatization of aldehydes.[20, 21] A key advantage of this DA is the incorporation of a bromophenethyl group, which introduces a distinctive isotopic signature of bromine to the derivative product ions. This helps with facilitating confident non-targeted detection and screening of derivatized compounds. In this work, we developed and optimized OTCD parameters for 4-APEBA deposition to enable simultaneous visualization and confident detection of unique phytohormones, amino acids, components of the glyoxylate cycle, glycosides, etc., which were not observed by MALDI-MSI without derivatization or with previously reported DAs.

Materials and methods

In-solution derivatization screening experiments

A stock solution of abscisic acid was created in water (3 mg/mL), where equimolar amounts of 1:100 dilution abscisic acid were aliquoted into glass vials with each respective DA. Additional solution was added to ensure constant volume and reaction conditions for each tested DA and were performed at a constant molar ratio of 1:80 of standard:DA. The reactions occurred at 37.5 °C for 16 hr. Exposure to high temperatures was not tested, as these conditions are not practical for translation to MALDI-MSI workflows with preservation of labile molecules. After the reaction was complete, the samples were diluted to 30 nmol/L and subsequently run by ESI. Several of these reactions were then profiled by dried droplet preparations for MALDI-MS.

In-situ derivatization of dried droplet standards

To validate the developed OTCD protocol described within the **Supporting Information,** several standards were spotted onto indium tin oxide (ITO)-coated glass slides (Bruker Daltonics, Billerica, MA) at 2 mmol/L and allowed to dry. Slides were then profiled using the MALDI-MSI method described, and subsequently the standards underwent tandem MS for the benchmarking of fragmentation behavior for MALDI-MSI analyses. As described in the **Supporting Information**, derivatization was further evaluated both with and without activation by 1-ethyl-3-(3-dimethylaminopropyl)carbodiimide (EDC) prior to deposition of 4-APEBA.

Plant tissue preparation for MALDI-MSI

Both frozen soybean root nodules and poplar roots (growth conditions described in the **Supporting Information**) were embedded within a mixture of 7.5% Hydroxypropyl methylcellulose (HPMC) and 2.5% polyvinylpyrrolidone (PVP).[22] These samples were cryosectioned at -10 °C using a CryoStar NX-70 Cryostat (Thermo Scientific, Runcorn, UK), and 12 µm sections were subsequently thaw-mounted onto ITO coated slides. Four sets of poplar root and soybean nodule sections were mounted onto each slide. Next to each pair of sections, a spot of 1 µL of 2 mmol/L abscisic acid (in 50% MeOH) was pipetted and allowed to dry as a quality control for OTCD. All plant tissues were imaged within one week of cryosectioning and were stored at -80 °C in vacuum sealed bags with desiccant until analyzed.

Mass Spectrometry Instrumentation

ESI screening of in-solution reactions was performed on a hybrid 21T Velos Pro FTICR mass spectrometer fitted with a Window Cell, which is located in the Environmental Molecular Sciences Laboratory at Pacific Northwest National Laboratory.[23] Acquisitions were acquired in triplicate over the *m/z* range of 150 to 1,000 in the positive ion mode with a transient of 0.768 s. The observed mass resolution was ~315k at *m/z* 400, and the compounds were identified with low ppb error.

All imaging was performed on a Bruker Daltonics 12T solariX FTICR MS, equipped with a ParaCell. This instrument has an Apollo II ESI and MALDI source with a SmartBeam II frequency-tripled (355 nm) Nd: YAG laser (Bremen, Germany). All sample preparation was completed on an M5 Sprayer (HTX Technologies, Chapel Hill, NC) with all methods described within the **Supporting Information.** Positive ion mode OTCD acquisitions were acquired with broadband excitation from *m/z* 98.3 to 1,000, resulting in a detected transient of 0.5593 s— the observed mass resolution was ~110k at *m/z* 400. Negative ion mode NEDC analyses were acquired with broadband excitation from *m/z* 98.3 to 1,100, resulting in a detected transient of 0.5593 s— the observed mass resolution was

~110k at *m/z* 400. Compounds were identified with low ppm error. FlexImaging (Bruker Daltonics, v.5.0) was used for the imaging experiments, and analyses were performed with 25 µm step size for poplar roots, 50 µm step size for soybean root nodules, and 100 µm step size for the were profiled spotted standards.

MALDI-MSI data processing

FlexImaging sequences were directly imported into SCiLS Lab (Bruker Daltonics, v.2023.a Premium 3D) using automatic MRMS settings. Ion images were directly processed from the profile datasets within SCiLS Lab, and automated annotation of the centroided dataset was completed within METASPACE with a chemical modifier corresponding to the mass shift expected from 4-APEBA derivatization (+ $C_{18}H_{22}N_2Br$, + 345.09663 Da). KEGG-v1 and BraChemDB-2018-01 were used as metabolite databases for annotations.

RESULTS AND DISCUSSION

Screening DAs with a model phytohormone reveals 4-APEBA outperforms the others

Phytohormones are incredibly diverse within physiological function and functional groups present within their structures.[24-27] We selected abscisic acid as a model target for phytohormone derivatization, because it contains both a carboxyl and carbonyl functional group **(Fig. 1a)**. We tested several DAs **(Fig. 1b)** that could potentially enhance abscisic acid ionization efficiency and, more importantly, would be amenable to on-tissue deposition. Aside from previously reported DAs for MALDI,[18, 28-30] we also synthesized and tested 4-APEBA and 3-bromoactonyltrimethylammonium bromide (BTA). BTA had previously showed potential in derivatizing acidic plant hormones for capillary electrophoresis-MS analyses.[31] As OTCD is more challenging than in-solution analyses, and dried droplet preparations for MALDI are highly variable,[32] these reagents were initially screened by ESI to identify stable DA product ions **(Figure 1c)**.

An ideal OTCD workflow should have a number of key attributes: (1) it should be performed under mild conditions, (2) provide a high reaction yield on-tissue, (3) prevent the delocalization of analytes, (4) preserve tissue integrity, and (5) provide robust and reproducible results.[12] Through these ESI experiments, we observed that 4-APEBA provided the greatest potential, with a significant sensitivity boost for derivatized abscisic acid, whereas BTA, GT, and DNPH provided enhancement, but were 1.6 to 2.9 log2-fold less responsive **(Fig. 1c)**. High derivatization yields for 4-APEBA, BTA, DNPH, and PA were also found, where non-derivatized abscisic acid was not detected for these DAs or was below the limit of detection. While GP and PA produced derivatized product ions under these mild conditions, the sensitivity boost was 4.2 and 4.3 log2-fold less than 4-APEBA, respectively. Conversely, N,N,N-trimethyl-2-(piperazin-1-yl)ethan-1-aminium iodide (TMPA) and N,N-dimethylpiperazine

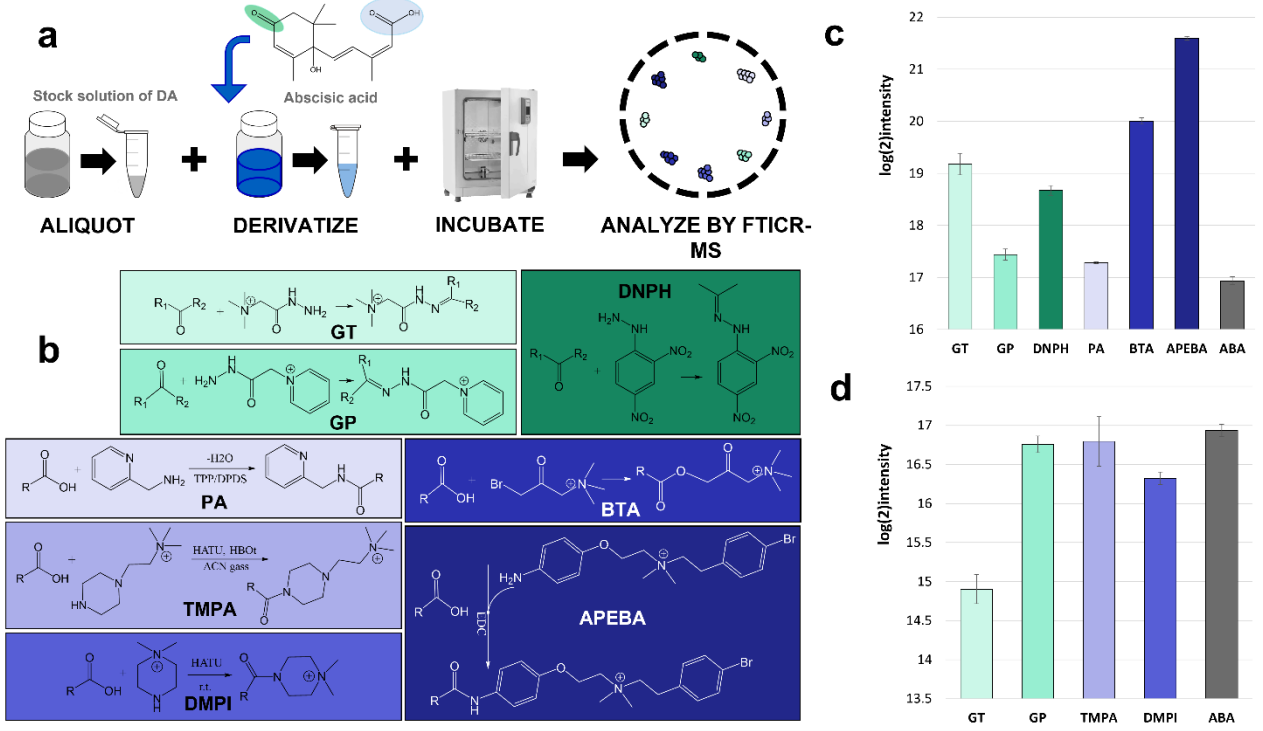

Fig. 1 Testing efficacy of various DAs by ESI-FTICR-MS. **a**) Workflow used for screening derivatization reactions using abscisic acid as a model phytohormone. **b**) Reaction scheme for all the DAs tested within this study and their respective color coding. **c**) Sensitivity boost due to derivatization noted within ESI-FTICR-MS measurements, where the signal intensity is log2 scaled for the different product ions of abscisic acid and compared against the abscisic acid standard. **d**) Relative intensity of non-derivatized abscisic acid detected across all reactions tested. If not listed, then abscisic acid was either fully reacted or below the limit of detection of the

iodide (DMPI) were found to be ineffective in the tested conditions, and negligible differences in signal intensity were observed for non-derivatized abscisic acid compared to non-derivatized control conditions **(Fig. 1d)**. In either case, where the non-derivatized or product ion was not detected, selective isolation and accumulation of a mass window around the ion was completed. However, even within these conditions these ions were not detected.

While the results for each of the eight in-solution DA trials will vary under different conditions, our data provided an first pass screening under mild conditions. For example, non-derivatized abscisic acid was detected for both GT and GP **(Fig. 1d)**, and even though a vast molar excess of DA was present (1:80), the reactions did not complete, which implies harsher conditions for derivatization are necessary. Additionally, several of the aforementioned DAs have previously been used for OTCD of carbonyl (DNPH[28]) and carboxyl containing metabolites (TMPA[29] and DMPI[30]). Nevertheless, as stated above, we opted to evaluate mild conditions and avoid prolonged incubation and exposures to high temperatures.

We then profiled a subset of high performing DAs within the initial screening to evaluate their potential for MALDI-MSI. Specifically, we tested both BTA and 4-APEBA and two commonly applied DAs, both GP and GT. Several single mass spectra were taken of dried droplet preparations for 4-APEBA, BTA, GP, and GT **(Fig. 2)**. Both 4-APEBA **(Fig. 2a)** and BTA **(Fig. 2b)** showed the highest sensitivity enhancement for the derivatization product ions within MALDI-MS experiments. Furthermore, 4-APEBA produced far fewer background peaks than all other DAs at a signal-to-noise threshold of 3 **(Fig. 2e)**. This is a notable advantage of 4-APEBA, as the number of spectral features from the other DAs poses a bioinformatics challenge for false annotation of ion images based solely on high-resolution accurate mass detection.

Recently, the development of an open cloud-based annotation platform for MSI datasets, METASPACE, has helped facilitate non-targeted analysis of MSI data.[33] Within METASPACE, complex mass spectral features are annotated using a false discovery rate (FDR) framework that tremendously improves confidence, while expediting annotation of spatially resolved MS data.[17] In tandem with lower background, the introduction of a bromine atom into the analyte from the bromophenethyl of the 4-APEBA **(Fig. 2a)** offers significantly higher confidence within METASPACE annotations, where ^{79}Br and ^{81}Br have distinct relative abundance and an easily recognizable

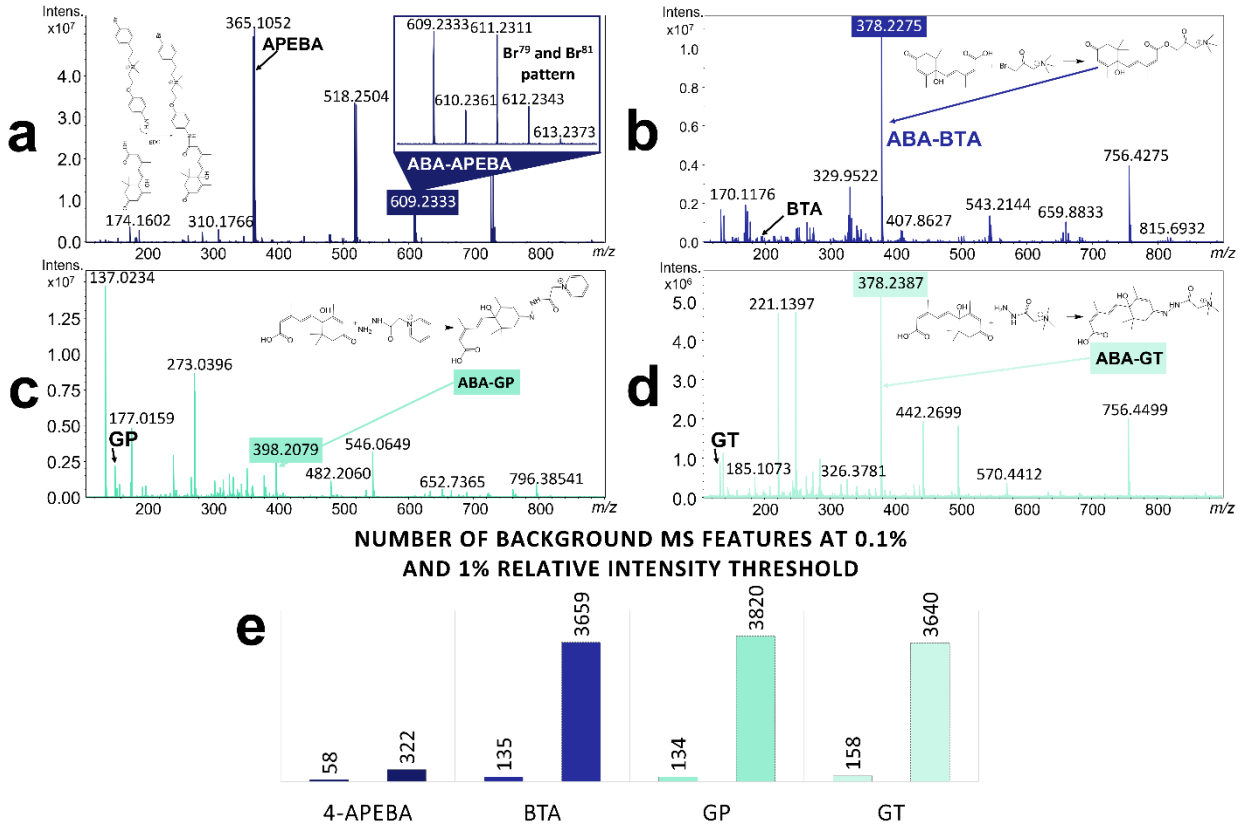

Fig. 2 MALDI mass spectra of different derivatization reactions of abscisic acid using DHB as a MALDI matrix. Experiments were completed to identify the expected background within a singular pixel in an imaging analysis. **a)** MALDI mass spectrum of derivatization reaction products using 4-APEBA. Note that within the zoomed inset, a bromine isotopic pattern can be discerned in the 4-APEBA abscisic acid product ion. **b)** MALDI mass spectrum of derivatization reaction products using BTA. **c)** MALDI mass spectrum of derivatization reaction products using GP. **d)** MALDI mass spectrum of derivatization reaction products using GT. **e)** Number of MS peaks with a signal-to-noise threshold of 3 at 1% and 0.1% relative intensity thresholds, where more complex signal background complicates downstream analyses.

isotopic pattern.[19] Thus 4-APEBA, and other halogenated DAs, reduce the likelihood of false derivatized annotations when tandem MS is not feasible for one of several reasons.[17]

Optimizing on-tissue chemical derivatization of 4-APEBA for high-fidelity MALDI-MSI

After an effective preliminary screening, we thoroughly evaluated protocols for OTCD using EDC and 4-APEBA, and we identified a two-step derivatization reaction was optimal. This separated the activation of carboxylic acids, using EDC, and subsequent derivatization by 4-APEBA. Consequently, we also evaluated the quantity of reactants for the ideal EDC/4-APE BA ratio and evaluated this within MSI analyses performed on poplar root and soybean root nodule sections. All conditions for OTCD that were tested are within **Table S1**. These datasets were evaluated against the METASPACE annotation quantity and quality, the sensitivity of derivatized product detection, and detectable signal delocalization **(Fig. 3)**. In general, we found that several classes of compounds can be simultaneously detected, some of which never previous reported by FTICR-MSI, and classes such as biogenic amines which remain non-derivatized with application of 4-APEBA were still detectable post OTCD. As such, we used these molecules as a sensitivity control to gauge DA suppression.

Signal delocalization **(Fig. 3a)** was quantified using our previously published procedure,[34] and all annotations were limited to those with FDRs <10% **(Fig. 3b)**. We found molecules annotated below this threshold consisted of mostly non-derivatized species and/or false positives. Low FDRs, in tandem with high metabolite-signal match (MSM)[33] and diagnostics in METASPACE **(Fig. 3d)**, enabled high confidence profiling of annotations. As a quality control for OTCD a standard of abscisic acid was spotted beside the tissue and profiled during the MALDI-MSI acquisition. We used the relative intensity of the derivatized abscisic acid product ion to calculate the sensitivity of each tested condition **(Fig. 3c)**. As such, the intensity reflects the mutual effect of derivatization yield and suppression caused by the MALDI matrix and DA.

Taken together we identified the optimal conditions, regardless of the plant tissue imaged, were obtained after depositing 16.66 µg/cm^2 of aqueous EDC followed by 5.56 µg/cm^2 of aqueous 4-APEBA within four spray cycles, as outlined within the methods in the **Supporting Information**. Subsequently, lower, or higher deposited amounts of EDC/4-APEBA, or combined spraying of EDC/4-APEBA, or a higher EDC/4-APEBA ratio caused unfavorable interactions on the sampled surface, which resulted in non-homogeneous matrix application, signal suppression, and delocalization. Interestingly, applying lower amounts of DAs also increased delocalization **(Fig. 3a)**. We found this result to be counterintuitive because higher amounts of deposited DA require several more application cycles with the matrix sprayer. We postulate that this observation could have resulted from low derivatization yield and ion suppression from other non-derivatized molecules.

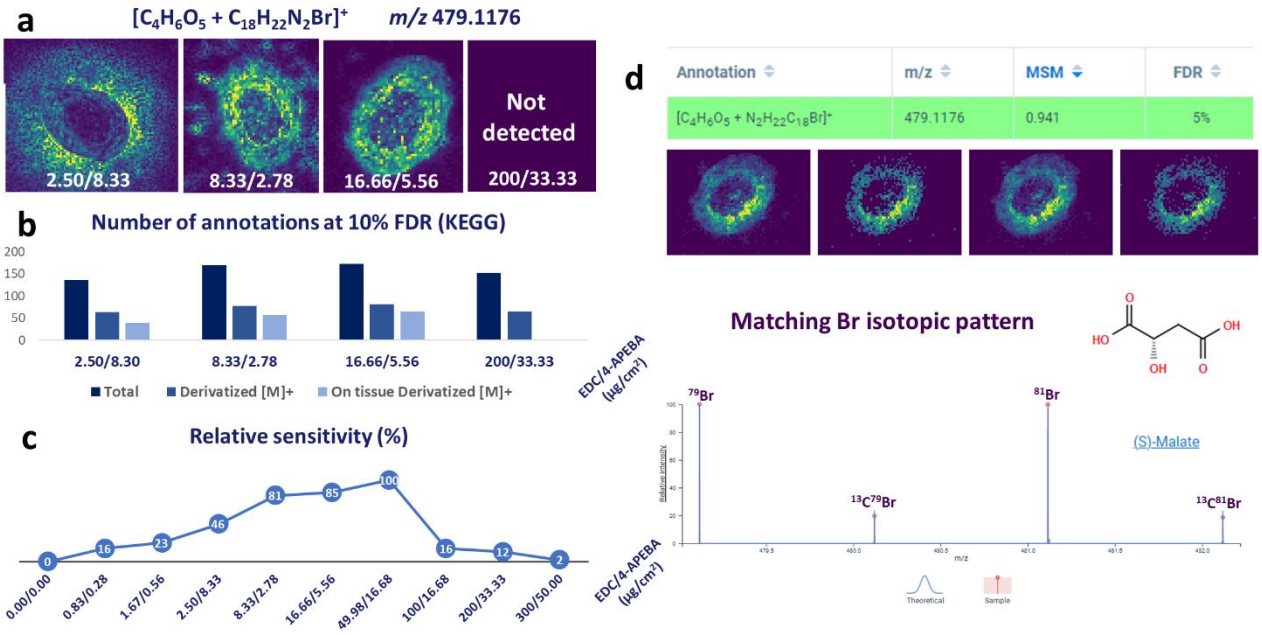

Fig. 3 MALDI-MSI outputs in different EDC/4-APEBA derivatization conditions expressed as EDC (µg/cm^2) / 4-APEBA (µg/cm^2) demonstrated on poplar root cross section. **a)** Delocalization (i.e., leakage of molecules from their native localizations) observed after deposition of EDC and APEBA in water on poplar roots. The derivatized form of malic acid $[C_4H_6O_5+C_{18}H_{22}N_2Br]^+$ is provided as an exemplary molecule used to evaluate delocalization. **b)** Number of annotated features retrieved from METASPACE at 10% FDR using KEGG database of these datasets. **c)** Sensitivity of analyses expressed as relative intensity of derivatized abscisic acid standard in each condition. **d)** Spatial distribution of $[malate\text{-}4\text{-}APEBA]^+$ isotopologues in the cross section of poplar root. Characteristic isotopic pattern of bromine (^{79}Br and ^{81}Br) can be identified with similar relative abundances (51% and 49%, respectively) aiding in spectral identification of isotopologues, which for low mass metabolites are otherwise broadly undetected.

We found sensitivity plateaued at our aforementioned optimal conditions **(Fig. 3c)**. We also tested using different solvent conditions, where OTCD was performed using 50% MeOH, **(Fig. S1)**. Generally, a differential sensitivity boost was observed for various metabolites (i.e., derivatized lipoate, glyoxylate, and formate) likely due to differential extraction. In comparison to the optimized aqueous protocol, we detected and annotated less phytocompounds. These results were also found to be specific to tissue type, with drastically less annotations on soybean root nodules with 50% MeOH **(Table S1)**. As such, our results demonstrate a critical need to also evaluate the solvent system for molecular coverage, sensitivity, delocalization, and DA stability when approaching targeted OTCD workflows.

The entire optimization was also performed using DHB as a matrix, which itself contains a carboxyl group that can be derivatized. Accordingly, a derivatized DHB product ion was a major product ion within these analyses alongside excess 4-APEBA. While this could impact ionization yields in an imaging experiment, for example, we also tested norharmane (NOR) as an OTCD matrix. This matrix has shown great utility within dual polarity MALDI-MSI.[35, 36] However, we found that both sensitivity and molecular coverage for OTCD with NOR deposition were significantly lower compared to DHB **(Fig. S2)**. These finding were further supported by ion images of non-derivatized components within DHB experiments **(Fig. S3)**, suggesting derivatization of DHB did not negatively impact sensitivity. Alternatively, DHB can act as a quality control to ensure efficient OTCD occurred.

Verification of on-tissue chemical derivatization workflows through evaluation of standards

For further verification of OTCD, several standards containing aldehyde and carboxylate functional groups were activated, derivatized, and analyzed as dried droplets on a slide with the optimized parameters **(Fig. S4)**. As we expected, all carboxyl-containing compounds showed intense derivatized signals, and their non-derivatized forms were either not detected or were detected with less than 11.5 log2-fold lower signal intensity. Notably, glucose showed a significantly enhanced derivatized signal with 5.2 log2-fold higher response than non-derivatized glucose **(Table S2)**, indicating that 4-APEBA in our conditions also targets aldehydes. On the other hand, it seems that glycosides were poorly derivatized, as derivatized zeatin riboside was a very minor component of zeatin riboside mass spectrum **(Fig. S4a)**. We also observed negligible double derivatization in molecules that contain multiple carboxyl groups (e.g., citric acid) within our analyses, but we did not detect double derivatization for any other molecules that have mixed chemical functionality (i.e., abscisic acid, jasmonic acid, and lignin model compounds), as shown in **Table S2**.

To further probe the effect of this key two-step activation with EDC, aromatic aldehydes produced in lignocellulose decay were analyzed with and without activation by EDC **(Fig. S4b)**. Without prior EDC deposition, the $[DHB+4\text{-}APEBA]^+$ product ion signal is significantly lower compared to two-step activation and derivatization. In contrast, all aldehyde standards tested showed intense derivatized product ions both with and without EDC deposition. Without EDC, signal intensities were 0.7 to 9.3 log2-fold higher compared to signal in the presence of EDC **(Table S2)**. However, regardless of the condition, all non-derivatized ions were observed at <10% relative intensity of the derivatized ions. We also found an unexpected derivatization product with standards of acetovanillone and hydroquinone. Namely, several peaks with low-ppm mass accuracy match to a 4-APEBA moiety attached to acetovanillone and hydroquinone after a water loss **(Fig. S4c)**. As acetovanillone is a ketone, this is plausible, but hydroquinone has two phenol groups and no carbonyls, it remains unclear the mechanism of derivatization by 4-APEBA, although oxidation of phenols is possible through several mechanisms.[37] Consequently, METASPACE annotations of other carbonyl or phenol compounds should not be directly excluded as false, but rather should be further investigated.

Overall, activation by EDC was found to be a necessary component for efficient derivatization of carboxylates with minor detrimental effects for other functional groups targeted that do not need activation.[20] These results signify a niche opportunity with DA specificity towards functional groups, which in the future can be exploited to image structural isomers by MALDI-MSI,[38] depending on the DA or sample preparation for OTCD.[39] MALDI tandem MS was also evaluated **(Fig. S5)**, where common neutral losses were identified **(Table S3)** and follow generalizations for neutral losses based upon the functional group derivatized.

On-tissue chemical derivatization by 4-APEBA enabled high-fidelity cellular mapping of phytohormones and phytochemicals

Finally, we applied our optimal 4-APEBA OTCD protocol to provide fine spatial information on more than 280 metabolites within plant tissue. Detailed insight into the identity of these molecules can be seen in the **Supplementary Workbook** and visualized via METASPACE. Besides the detection of important physiological aldehydes, and carboxylic acids, this approach provided broad detection of molecules of different chemistries, polarities, and physiological roles within a single MSI experiment. To date, to obtain similar coverage and visualize

aldehydes, and carboxylic acids, one either needs to use multiple DAs, which are each specific for a unique functional group,[18] or prepare multiple tissue sections for separate imaging experiments in opposite polarities.

To exemplify the multiplexed capability of 4-APEBA OTCD, we highlight the spatial pattern of the critical respiratory substrate, pyruvate,[40] its decarboxylation product, acetaldehyde,[41] and stress reporter, glyoxylate **(Fig. 4).**[42] Due to their low molecular weights (88 Da, 44 Da, and 74 Da, respectively) these small metabolites have remained undetected in MSI experiments performed with FTICR-MS thus far. It is worth noting that using PA for OTCD, pyruvate was previously ascribed with a neutral loss [-CO_2] in the positive ion mode.[18] In this report, it was annotated as an acetaldehyde-PA product ion, but since acetaldehyde is volatile, it was postulated that it was unlikely to be preserved in the plant tissue.[18] Other studies have annotated pyruvate in the negative ion mode within root nodules.[43] However, these works and others to date used low-resolving power instrumentation for such measurements. While highly informative, lower mass accuracy and mass resolving power limits the confidence of molecular annotations. Regardless, our results show, for the first time, a direct, clear, and confident image of pyruvate distribution in the tissue **(Fig. 4a)**. This is invaluable in tracking pyruvate kinetics in plants during respiration as an intermediary through glycolysis into gluconeogenesis. Other small aliphatic acids that are part of the TCA and glyoxalate cycles in plant were also observed, including cis-aconitate, α-ketoglutarate, fumarat e, citrate/iso-citrate, malate, and succinate **(Fig. 4a)** allowing for comprehensive metabolic pathway profiling.[44]

We were also able to detect derivatized aliphatic acids with specific biological roles, such as allantonate, that serve as long-distance nitrogen transporters in soybean nodules **(Fig. 4b)**.[45] Numerous flavonol glycosides were also derivatized and detected with unique spatial distributions. This included malonyl-containing flavonol glycoside, which was concentrated at the area of root attachment in the soybean root nodule **(Fig. 4b)**. We also detected malonate in soybean root nodules **(Fig. 4b)**. Malonate is an abundant C3-dicarboxylic acid in legumes,

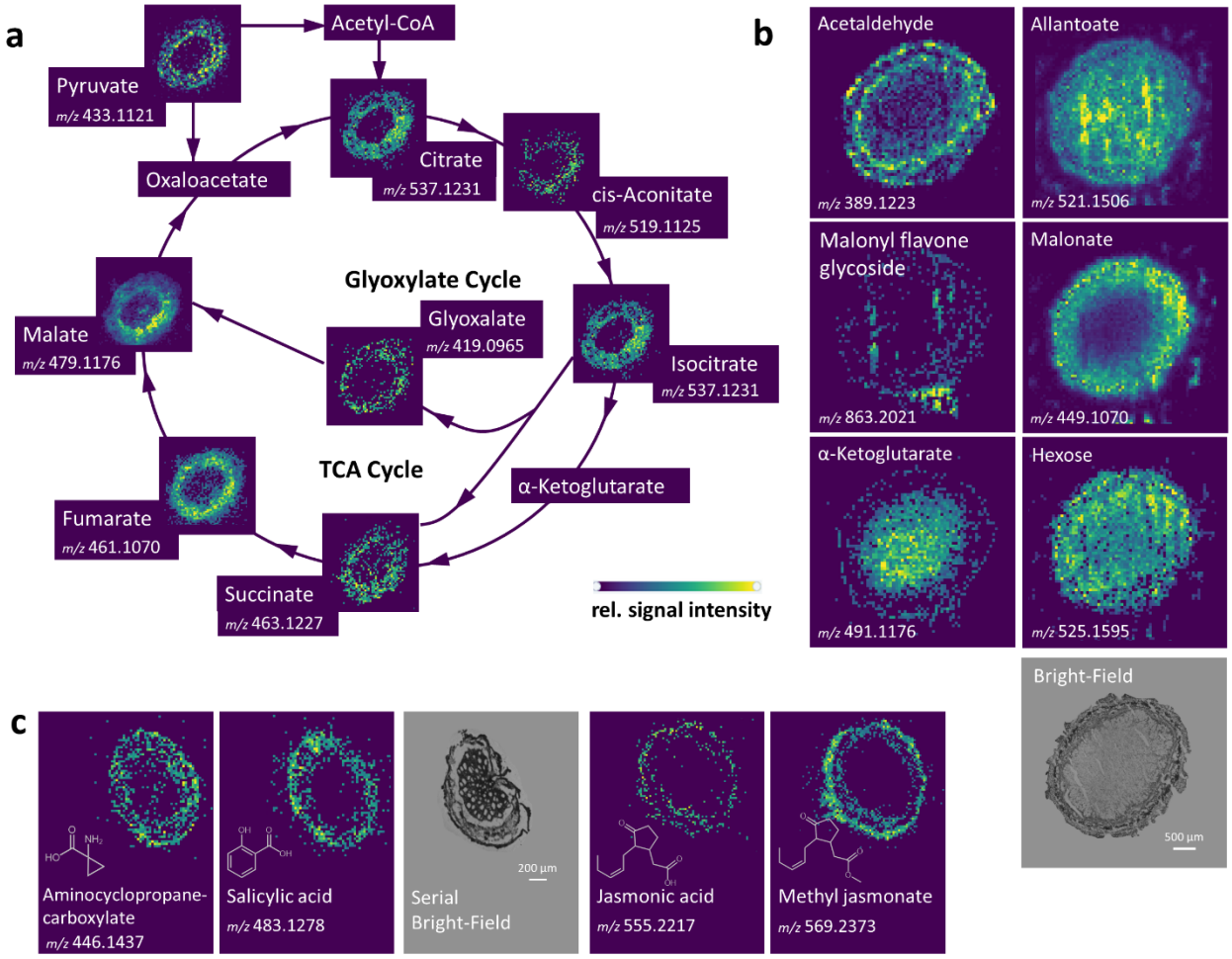

Fig. 4 Spatial distribution of exemplary plant metabolites revealed after on-tissue derivatization with 4-APEBA. All ions were detected as 4-APEBA derivative ion $[M+C_{18}H_{22}N_2Br]^+$. **a)** Spatial distribution of multiple components of the TCA and glyoxalate cycle in the cross section of poplar root at 25 µm pixel size. **b)** Cell-type specific localization of selected metabolites in the soybean root nodule at 50 µm spatial scale where localizations within the cortex and outer dermal layers can be recognized. A bright-field image of the imaged section is shown. **c)** MALDI images of phytohormone distribution in soybean root nodule (right: jasmonic acid and methyl jasmonate) and poplar roots (left: salicylate and 1-aminocyclopropane-1-carboxylate). A bright-field image of a serial section to that which was imaged is shown.

and its role in biological nitrogen fixation is highly contested (*i.e.,* from a significant carbon source to a metabolic poison).[46] Importantly, this metabolite has not been observed within soybean root nodules via several different MSI capable methods previously used,[47-49] nor was it detected in other legume nodules.[43] Revealing high abundance of malonate in the outer layer of the infection zone may shed new light on its role in biological nitrogen fixation. The sensitivity of 4-APEBA OTCD also allowed visualization of other important phytocompounds, such as phytohormones and growth regulators,[50] which have been largely undetectable by all MSI methods. For example, we showed the distribution of abscisic acid **(Fig. S6)**,[51] aminocyclopropane-carboxylate,[52] and salicylic acid[53] in poplar roots **(Fig. 4c),** and abscisic acid, jasmonic acid, and methyl jasmonate[54] in soybean root nodules **(Fig. 4c)**.

This demonstrates the vast potential of 4-APEBA as a DA that enables detection of key phytocompounds, including phytohormones that are often present only in the trace amounts in individual cells. Routine non-targeted detection of these vital signaling molecules has not been feasible until now, even when state-of-the-art analytical techniques were employed.[50, 55] Under optimal conditions, we can even measure non-derivatized molecules **(Fig. S3)** — albeit with less sensitivity than in conditions where the sample has not been derivatized. Thus, analyses are not limited solely to carboxyl, and aldehyde containing molecules from the derivatized tissue, as biogenic amines in soybean nodules that are synthesized by rhizobia to adapt to the plant cell environment can also be detected **(Fig. S3)**.[56]

Finally, we compared the utility of 4-APEBA OTCD to profile carbonyls against negative ion mode experiments that are the primary choice for these molecules. Several compounds (30) detected by 4-APEBA can still be visualized within negative ion mode using NEDC as a matrix, with similar spatial distributions **(Fig. S7)**. However, 4-APEBA molecular coverage vastly outperforms NEDC analyses **(Table S4)** and opens a door for imaging numerous aliphatic carbonyls not detectable by traditional negative mode measurements (**Fig. S8**).

Conclusions

OTCD methods are still in their infancy. However, over the last half decade, innovations in DAs and deposition methods have dramatically increased the metabolic coverage that can be obtained at the cellular spatial scale using MSI methods. This study provides a derivatization methodology using a highly promising OTCD agent, 4-APEBA, that enabled simultaneous boosts in sensitivity for amino acids, hormones, reducing sugars, aliphatic and aromatic carboxylic acids, aldehydes, and other metabolites with carbonyl groups. This DA has an extremely low background and the incorporation of polyisotopic bromine into the derivative product ion, the combination of which facilitates confident bioinformatics processing. The optimized workflow demonstrates these analyses can occur at the cellular scale, where any delocalization identified is an artifact of stemming from tissue embedding procedures.

Although we demonstrated the applicability of 4-APEBA in plant root tissues, this approach is transferrable to microbial colonies, mammalians tissues, and other biological systems as well. The two-step reaction within OTCD also revealed further potential development for selective derivatization of aldehydes, and plausibly other carbonyls, whereas detection of carboxyl groups require prior activation for sensitive analyses. Regardless, within a single imaging analysis, metabolites of opposite polarities and different hydrophobicity can be detected with negligible double derivatizations observed. In summary, having demonstrated the *in-situ* profiling of key phytocompounds and metabolites, the path forward for sensitive spatial metabolomics and hormonomics is promising. Especially due to limited reports detailing detection of several of these biologically important compounds and incomplete coverage of metabolic pathways.

ASSOCIATED CONTENT

Supporting Information

Supporting information containing extended methods, figures, and tables (.docx)

Workbook containing METASPACE annotations from all presented MALDI-MSI datasets (.xslx)

AUTHOR INFORMATION

Corresponding Author

*Dušan Veličković – Environmental and Biological Sciences Directorate, Pacific Northwest National Laboratory, Richland, Washington 99354, United States

Email: dusan.velickovic@pnnl.gov

Author Contributions

D.V. conceptualized and supervised the project. K.J.Z. performed derivatization and MALDI-MSI experiments. K.J.Z. and D.V. performed data analysis and visualization. V.L. synthesized derivatization agents. A.A. and T.W. generated and provided poplar plants. D.V. acquired funding for the project. K.J.Z. and D.V. wrote the initial manuscript with V.L., A.A., T.W., and C.R.A. providing input. All authors edited the manuscript.

Notes

All annotations and ion images can be found in the following METASPACE project:

https://metaspace2020.eu/api_auth/review?prj=f8500888-401a-11ed-89bf-4f62674f048b&token=JvizK2A5QuJo

ACKNOWLEDGMENT

This research was performed on a project award doi.org/10.46936/intm.proj.2021.60091/60001441 (D.V.) from the Environmental Molecular Sciences Laboratory, a Department of Energy (DOE) Office of Science User Facility sponsored by the Biological and Environmental Research program under Contract No. DE-AC05-76RL01830.

REFERENCES

1. Fang, C. Y.; Fernie, A. R.; Luo, J., Exploring the Diversity of Plant Metabolism. *Trends Plant Sci* **2019,** *24* (1), 83-98.

2. Katam, R.; Lin, C. W.; Grant, K.; Katam, C. S.; Chen, S. X., Advances in Plant Metabolomics and Its Applications in Stress and Single-Cell Biology. *Int J Mol Sci* **2022,** *23* (13).

3. de Souza, L. P.; Borghi, M.; Fernie, A., Plant Single-Cell Metabolomics-Challenges and Perspectives. *Int J Mol Sci* **2020,** *21* (23).

4. Taylor, M. J.; Lukowski, J. K.; Anderton, C. R., Spatially Resolved Mass Spectrometry at the Single Cell: Recent Innovations in Proteomics and Metabolomics. *J Am Soc Mass Spectr* **2021,** *32* (4), 872-894.

5. Velickovic, D.; Ropartz, D.; Guillon, F.; Saulnier, L.; Rogniaux, H., New insights into the structural and spatial variability of cell-wall polysaccharides during wheat grain development, as revealed through MALDI mass spectrometry imaging. *J Exp Bot* **2014,** *65* (8), 2079-2091.

6. Velickovic, D.; Liao, Y. C.; Thibert, S.; Velickovic, M.; Anderton, C.; Voglmeir, J.; Stacey, G.; Zhou, M. W., Spatial Mapping of Plant N-Glycosylation Cellular Heterogeneity Inside Soybean Root Nodules Provided Insights Into Legume-Rhizobia Symbiosis. *Front Plant Sci* **2022,** *13*.

7. Sturtevant, D.; Aziz, M.; Romsdahl, T. B.; Corley, C. D.; Chapman, K. D., In Situ Localization of Plant Lipid Metabolites by Matrix-Assisted Laser Desorption/Ionization Mass Spectrometry Imaging (MALDI-MSI). *Methods Mol Biol* **2021,** *2295*, 417-438.

8. Liu, H. Q.; Han, M. M.; Li, J. M.; Qin, L.; Chen, L. L.; Hao, Q. C.; Jiang, D. X.; Chen, D. F.; Ji, Y. Y.; Han, H.; Long, C. L.; Zhou, Y. J.; Feng, J. C.; Wang, X. D., A Caffeic Acid Matrix Improves In Situ Detection and Imaging of Proteins with High Molecular Weight Close to 200,000 Da in Tissues by Matrix-Assisted Laser Desorption/Ionization Mass Spectrometry Imaging. *Anal Chem* **2021,** *93* (35), 11920-11928.

9. Zhou, M.; Fulcher, J. M.; Zemaitis, K. J.; J, D. D.; Y-C, L.; Velickovic, M.; Velickovic, D.; Bramer, L.; Kew, W. R.; Stacey, G.; Pasa-Tolic, L., Discovery top-down proteomics in symbiotic soybean root nodules. *Front. Anal. Sci.* **2022,** *2*, 1012707.

10. Dong, Y. H.; Sonawane, P.; Cohen, H.; Polturak, G.; Feldberg, L.; Avivi, S. H.; Rogachev, I.; Aharoni, A., High mass resolution, spatial metabolite mapping enhances the current plant gene and pathway discovery toolbox. *New Phytol* **2020,** *228* (6), 1986-2002.

11. Velickovic, D.; Liao, H. L.; Vilgalys, R.; Chu, R. K.; Anderton, C. R., Spatiotemporal Transformation in the Alkaloid Profile of Pinus Roots in Response to Mycorrhization. *J Nat Prod* **2019,** *82* (5), 1382-1386.

12. Merdas, M.; Lagarrigue, M.; Vanbellingen, Q.; Umbdenstock, T.; Da Violante, G.; Pineau, C., On-tissue chemical derivatization reagents for matrix-assisted laser desorption/ionization mass spectrometry imaging. *J Mass Spectrom* **2021,** *56* (10).

13. Harkin, C.; Smith, K. W.; Cruickshank, F. L.; Mackay, C. L.; Flinders, B.; Heeren, R. M. A.; Moore, T.; Brockbank, S.; Cobice, D. F., On-tissue chemical derivatization in mass spectrometry imaging. *Mass Spectrom Rev* **2021**.

14. Zhou, Q. Q.; Fulop, A.; Hopf, C., Recent developments of novel matrices and on-tissue chemical derivatization reagents for MALDI-MSI. *Anal Bioanal Chem* **2021,** *413* (10), 2599-2617.

15. Yang, H.; Chandler, C. E.; Jackson, S. N.; Woods, A. S.; Goodlett, D. R.; Ernst, R. K.; Scott, A. J., On-Tissue Derivatization of Lipopolysaccharide for Detection of Lipid A Using MALDI-MSI. *Anal Chem* **2020,** *92* (20), 13667-13671.

16. Dreisbach, D.; Heiles, S.; Bhandari, D. R.; Petschenka, G.; Spengler, B., Molecular Networking and On-Tissue Chemical Derivatization for Enhanced Identification and Visualization of Steroid Glycosides by MALDI Mass Spectrometry Imaging. *Analytical Chemistry* **2022,** *94* (46), 15971-15979.

17. Larson, E. A.; Forsman, T. T.; Stuart, L.; Alexandrov, T.; Lee, Y. J., Rapid and Automatic Annotation of Multiple On-Tissue Chemical Modifications in Mass Spectrometry Imaging with Metaspace. *Anal Chem* **2022,** *94* (25), 8983-8991.

18. Duenas, M. E.; Larson, E. A.; Lee, Y. J., Toward Mass Spectrometry Imaging in the Metabolomics Scale: Increasing Metabolic Coverage Through Multiple On-Tissue Chemical Modifications. *Front Plant Sci* **2019,** *10*.

19. Shariatgorji, R.; Nilsson, A.; Strittmatter, N.; Vallianatou, T.; Zhang, X. Q.; Svenningsson, P.; Goodwin, R. J. A.; Andren, P. E., Bromopyrylium Derivatization Facilitates Identification by Mass Spectrometry Imaging of Monoamine Neurotransmitters and Small Molecule Neuroactive Compounds. *J Am Soc Mass Spectr* **2020,** *31* (12), 2553-2557.

20. Eggink, M.; Wijtmans, M.; Kretschmer, A.; Kool, J.; Lingeman, H.; de Esch, I. J. P.; Niessen, W. M. A.; Irth, H., Targeted LC-MS derivatization for aldehydes and carboxylic acids with a new derivatization agent 4-APEBA. *Anal Bioanal Chem* **2010,** *397* (2), 665-675.

21. Kretschmer, A.; Giera, M.; Wijtmans, M.; de Vries, L.; Lingeman, H.; Irth, H.; Niessen, W. M. A., Derivatization of carboxylic acids with 4-APEBA for detection by positive-ion LC-ESI-MS(/MS) applied for the analysis of prostanoids and NSAID in urine. *J Chromatogr B* **2011,** *879* (17-18), 1393-1401.

22. Dannhorn, A.; Kazanc, E.; Ling, S.; Nikula, C.; Karali, E.; Serra, M. P.; Vorng, J.-L.; Inglese, P.; Maglennon, G.; Hamm, G.; Swales, J.; Strittmatter, N.; Barry, S. T.; Sansom, O. J.; Poulogiannis, G.; Bunch, J.; Goodwin, R. J. A.; Takats, Z., Universal Sample Preparation Unlocking Multimodal Molecular Tissue Imaging. *Analytical Chemistry* **2020,** *92* (16), 11080-11088.

23. Shaw, J. B.; Lin, T.-Y.; Leach, F. E.; Tolmachev, A. V.; Tolić, N.; Robinson, E. W.; Koppenaal, D. W.; Paša-Tolić, L., 21 Tesla Fourier Transform Ion Cyclotron Resonance Mass Spectrometer Greatly Expands Mass Spectrometry Toolbox. *Journal of The American Society for Mass Spectrometry* **2016,** *27* (12), 1929-1936.

24. Ogawa, S.; Cui, S. K.; White, A. R. F.; Nelson, D. C.; Yoshida, S.; Shirasu, K., Strigolactones are chemoattractants for host tropism in Orobanchaceae parasitic plants. *Nat Commun* **2022,** *13* (1).

25. Jing, H. W.; Korasick, D. A.; Emenecker, R. J.; Morffy, N.; Wilkinson, E. G.; Powers, S. K.; Strader, L. C., Regulation of AUXIN RESPONSE FACTOR condensation and nucleo-cytoplasmic partitioning. *Nat Commun* **2022,** *13* (1).

26. Zhu, T. T.; Herrfurth, C.; Xin, M. M.; Savchenko, T.; Feussner, I.; Goossens, A.; De Smet, I., Warm temperature triggers JOX and ST2A-mediated jasmonate catabolism to promote plant growth. *Nat Commun* **2021,** *12* (1).

27. Kokla, A.; Leso, M.; Zhang, X.; Simura, J.; Serivichyaswat, P. T.; Cui, S. K.; Ljung, K.; Yoshida, S.; Melnyk, C. W., Nitrogen represses haustoria formation through abscisic acid in the parasitic plant Phtheirospermum japonicum. *Nat Commun* **2022,** *13* (1).

28. Flinders, B.; Morrell, J.; Marshall, P. S.; Ranshaw, L. E.; Clench, M. R., The use of hydrazine-based derivatization reagents for improved sensitivity and detection of carbonyl containing compounds using MALDI-MSI. *Anal Bioanal Chem* **2015,** *407* (8), 2085-2094.

29. Sun, C.; Liu, W.; Geng, Y.; Wang, X., On-Tissue Derivatization Strategy for Mass Spectrometry Imaging of Carboxyl-Containing Metabolites in Biological Tissues. *Anal Chem* **2020,** *92* (18), 12126-12131.

30. Wang, S. S.; Wang, Y. J.; Zhang, J.; Sun, T. Q.; Guo, Y. L., Derivatization Strategy for Simultaneous Molecular Imaging of Phospholipids and Low-Abundance Free Fatty Acids in Thyroid Cancer Tissue Sections. *Anal Chem* **2019,** *91* (6), 4070-4076.

31. Chen, M. L.; Huang, Y. Q.; Liu, J. Q.; Yuan, B. F.; Feng, Y. Q., Highly sensitive profiling assay of acidic plant hormones using a novel mass probe by capillary electrophoresis-time of flight-mass spectrometry. *J Chromatogr B* **2011,** *879* (13-14), 938-944.

32. Choi, Y. K.; Oh, J. Y.; Han, S. Y., Large-Area Graphene Films as Target Surfaces for Highly Reproducible Matrix-Assisted Laser Desorption Ionization Suitable for Quantitative Mass Spectrometry. *J Am Soc Mass Spectr* **2018,** *29* (10), 2003-2011.

33. Palmer, A.; Phapale, P.; Chernyavsky, I.; Lavigne, R.; Fay, D.; Tarasov, A.; Kovalev, V.; Fuchser, J.; Nikolenko, S.; Pineau, C.; Becker, M.; Alexandrov, T., FDR-controlled metabolite annotation for high-resolution imaging mass spectrometry. *Nature Methods* **2017,** *14* (1), 57-60.

34. Velickovic, D.; Sharma, K.; Alexandrov, T.; Hodgin, J. B.; Anderton, C. R., Controlled Humidity Levels for Fine Spatial Detail Information in Enzyme-Assisted N-Glycan MALDI MSI. *J Am Soc Mass Spectr* **2022,** *33* (8), 1577-1580.

35. Treu, A.; Rompp, A., Matrix ions as internal standard for high mass accuracy matrix-assisted laser desorption/ionization mass spectrometry imaging. *Rapid Commun Mass Sp* **2021,** *35* (16).

36. Vandenbosch, M.; Nauta, S. P.; Svirkova, A.; Poeze, M.; Heeren, R. M. A.; Siegel, T. P.; Cuypers, E.; Marchetti-Deschmann, M., Sample preparation of bone tissue for MALDI-MSI for forensic and (pre)clinical applications. *Anal Bioanal Chem* **2021,** *413* (10), 2683-2694.

37. Pinnataip, R.; Lee, B. P., Oxidation Chemistry of Catechol Utilized in Designing Stimuli-Responsive Adhesives and Antipathogenic Biomaterials. *Acs Omega* **2021,** *6* (8), 5113-5118.

38. Takeo, E.; Sugiura, Y.; Uemura, T.; Nishimoto, K.; Yasuda, M.; Sugiyama, E.; Ohtsuki, S.; Higashi, T.; Nishikawa, T.; Suematsu, M.; Fukusaki, E.; Shimma, S., Tandem Mass Spectrometry Imaging Reveals Distinct Accumulation Patterns of Steroid Structural Isomers in Human Adrenal Glands. *Analytical Chemistry* **2019,** *91* (14), 8918-8925.

39. Velickovic, D.; Zhou, M. W.; Schilling, J. S.; Zhang, J. W., Using MALDI-FTICR-MS Imaging to Track Low-Molecular-Weight Aromatic Derivatives of Fungal Decayed Wood. *J Fungi* **2021,** *7* (8).

40. Millar, A. H.; Whelan, J.; Soole, K. L.; Day, D. A., Organization and Regulation of Mitochondrial Respiration in Plants. *Annu Rev Plant Biol* **2011,** *62*, 79-104.

41. Ventura, I.; Brunello, L.; Iacopino, S.; Valeri, M. C.; Novi, G.; Dornbusch, T.; Perata, P.; Loreti, E., Arabidopsis phenotyping reveals the importance of alcohol dehydrogenase and pyruvate decarboxylase for aerobic plant growth. *Sci Rep-Uk* **2020,** *10* (1).

42. Zarei, A.; Brikis, C. J.; Bajwa, V. S.; Chiu, G. Z.; Simpson, J. P.; DeEll, J. R.; Bozzo, G. G.; Shelp, B. J., Plant Glyoxylate/Succinic Semialdehyde Reductases: Comparative Biochemical Properties, Function during Chilling Stress, and Subcellular Localization. *Front Plant Sci* **2017,** *8*.

43. Ye, H.; Gemperline, E.; Venkateshwaran, M.; Chen, R. B.; Delaux, P. M.; Howes-Podoll, M.; Ane, J. M.; Li, L. J., MALDI mass spectrometry-assisted molecular imaging of metabolites during nitrogen fixation in the Medicago truncatula-Sinorhizobium meliloti symbiosis. *Plant J* **2013,** *75* (1), 130-145.

44. Zhang, Y. J.; Fernie, A. R., On the role of the tricarboxylic acid cycle in plant productivity. *J Integr Plant Biol* **2018,** *60* (12), 1199-1216.

45. Thu, S. W.; Lu, M. Z.; Carter, A. M.; Collier, R.; Gandin, A.; Sitton, C. C.; Tegeder, M., Role of ureides in source-to-sink transport of photoassimilates in non-fixing soybean. *J Exp Bot* **2020,** *71* (15), 4495-4511.

46. Karunakaran, R.; East, A. K.; Poole, P. S., Malonate Catabolism Does Not Drive N-2 Fixation in Legume Nodules. *Appl Environ Microb* **2013,** *79* (14), 4496-4498.

47. Agtuca, B. J.; Stopka, S. A.; Evans, S.; Samarah, L.; Liu, Y.; Xu, D.; Stacey, M. G.; Koppenaal, D. W.; Pasa-Tolic, L.; Anderton, C. R.; Vertes, A.; Stacey, G., Metabolomic profiling of wild-type and mutant soybean root nodules using laser-ablation electrospray ionization mass spectrometry reveals altered metabolism. *Plant J* **2020,** *103* (5), 1937-1958.

48. Samarah, L. Z.; Khattar, R.; Tran, T. H.; Stopka, S. A.; Brantner, C. A.; Parlanti, P.; Velickovic, D.; Shaw, J. B.; Agtuca, B. J.; Stacey, G.; Pasa-Tolic, L.; Tolic, N.; Anderton, C. R.; Vertes, A., Single-Cell Metabolic Profiling: Metabolite Formulas from Isotopic Fine Structures in Heterogeneous Plant Cell Populations. *Anal Chem* **2020,** *92* (10), 7289-7298.

49. Velickovic, D.; Agtuca, B. J.; Stopka, S. A.; Vertes, A.; Koppenaal, D. W.; Paga-Tolic, L.; Stacey, G.; Anderton, C. R., Observed metabolic asymmetry within soybean root nodules reflects unexpected complexity in rhizobacteria-legume metabolite exchange. *Isme J* **2018,** *12* (9), 2335-2338.

50. Wang, Y. H.; Irving, H. R., Developing a model of plant hormone interactions. *Plant Signal Behav* **2011,** *6* (4), 494-500.

51. Yu, D.; Wildhagen, H.; Tylewicz, S.; Miskolczi, P. C.; Bhalerao, R. P.; Polle, A., Abscisic acid signalling mediates biomass trade-off and allocation in poplar. *New Phytologist* **2019,** *223* (3), 1192-1203.

52. Polko, J. K.; Kieber, J. J., 1-Aminocyclopropane 1-Carboxylic Acid and Its Emerging Role as an Ethylene-Independent Growth Regulator. *Front Plant Sci* **2019,** *10*.

53. Ullah, C.; Tsai, C.-J.; Unsicker, S. B.; Xue, L.; Reichelt, M.; Gershenzon, J.; Hammerbacher, A., Salicylic acid activates poplar defense against the biotrophic rust fungus Melampsora larici-populina via increased biosynthesis of catechin and proanthocyanidins. *New Phytologist* **2019,** *221* (2), 960-975.

54. Zdyb, A.; Demchenko, K.; Heumann, J.; Mrosk, C.; Grzeganek, P.; Göbel, C.; Feussner, I.; Pawlowski, K.; Hause, B., Jasmonate biosynthesis in legume and actinorhizal nodules. *New Phytologist* **2011,** *189* (2), 568-579.

55. Wang, L. Y.; Zou, Y. L.; Kaw, H. Y.; Wang, G.; Sun, H. Z.; Cai, L.; Li, C. Y.; Meng, L. Y.; Li, D. H., Recent developments and emerging trends of mass spectrometric methods in plant hormone analysis: a review. *Plant Methods* **2020,** *16* (1).

56. Fujihara, S., Biogenic Amines in Rhizobia and Legume Root Nodules. *Microbes Environ* **2009,** *24* (1), 1-13.

TOC Graphic: